Protein Science (1996), *5*:422–433. Cambridge University Press. Printed in the USA.

Synthesis, structure, and structure–activity relationships of divalent thrombin inhibitors containing an α-keto-amide transition-state mimetic

RAMAN KRISHNAN,[1] A. TULINSKY,[1] GEORGE P. VLASUK,[2] DANIEL PEARSON,[2] PUREZA VALLAR,[2] PETER BERGUM,[2] TERENCE K. BRUNCK,[2] AND WILLIAM C. RIPKA[2]

[1] Department of Chemistry, Michigan State University, East Lansing, Michigan 48824-1322
[2] Corvas International, Inc., San Diego, California 92121

(RECEIVED July 24, 1995; ACCEPTED December 1, 1995)

Abstract

A new class of divalent thrombin inhibitors is described that contains an α-keto-amide transition-state mimetic linking an active site binding group and a group that binds to the fibrinogen-binding exosite. The X-ray crystallographic structure of the most potent member of this new class, CVS995, shows many features in common with other divalent thrombin inhibitors and clearly defines the transition-state-like binding of the α-keto-amide group. The structure of the active site part of the inhibitor shows a network of water molecules connecting both the side-chain and backbone atoms of thrombin and the inhibitor. Direct peptide analogues of the new transition-state-containing divalent thrombin inhibitors were compared using in vitro assays of thrombin inhibition. There was no direct correlation between the binding constants of the peptides and their α-keto-amide counterparts. The most potent α-keto-amide inhibitor, CVS995, with a $K_i = 1$ pM, did not correspond to the most potent divalent peptide and contained a single amino acid deletion in the exosite binding region with respect to the equivalent region of the natural thrombin inhibitor hirudin. The interaction energies of the active site, transition state, and exosite binding regions of these new divalent thrombin inhibitors are not additive.

Keywords: α-keto-amide; divalent inhibitors; transition state; X-ray crystallographic structure

Thrombin, a multifunctional serine protease, is important in hemostasis and thrombosis, eliciting both procoagulant effects by its action on fibrinogen to release fibrin and anticoagulant effects by virtue of its activation of Protein C (Sadler et al., 1993; Mann, 1994). Thrombin also exerts a bioregulatory function on platelet activation (Maraganore, 1993) by the proteolytic cleavage of a seven-transmembrane "thrombin receptor" found on specific cell types (Coughlin, 1994; Wilcox et al., 1994). The recognition of macromolecular substrates and certain naturally occurring protein inhibitors by thrombin is known to involve multiple molecular recognition sites (Tulinsky & Qui, 1993). Representative of this is the inhibitor hirudin, isolated from the salivary glands of the leech *Hirudo medicinalis* (Markwardt, 1989), which has specific interactions at both the catalytic site of thrombin as well as a spatially distinct (40 Å from the catalytic site) recognition binding exosite (Grutter et al., 1990; Rydel et al., 1990, 1991) referred to as the fibrinogen binding site or anion binding exosite (Fenton, 1981, 1986). The specific hirudin ionic and hydrophobic contacts utilized by the thrombin FBS are at its carboxy-terminus and include residues Asp 55′–Glu 65′ (Table 1). These residues are linked via a short segment (residues Gly 49′–Gly 54′) to an amino-terminal domain (residues 1′–48′) that sterically blocks access to the active sites. Interestingly, hirudin lacks the specific P1 basic residue that would normally occupy the S1 specificity pocket of this class of serine proteases.

In an effort to mimic hirudin's multivalent binding to thrombin in smaller molecules, synthetic inhibitors have been reported that incorporate a more typical active site-specific tripeptide amino-terminal binding region bound in an antiparallel β-sheet motif (DiMaio et al., 1990; Maraganore et al., 1990), and possessing, unlike hirudin, a basic P1 residue that is linked with a variety of bridging sequences (Szewczuk et al., 1992, 1993) to

Reprint requests to: William C. Ripka, Corvas International, Inc., 3030 Science Park Road, San Diego, California 92121; e-mail: wcripka@crash.cts.com.

Abbreviations: FBS, fibrinogen binding site; PP, 2-propylpentanoyl; Boc, butyloxycarbonyl; DCM, dichloromethane; HF, hydrofluoric acid; TFA, trifluoroacetic acid; FAB, fast atom bombardment; THF, tetrahydrofuran; BSA, bovine serum albumin; HBSA, Hepes-buffered saline with BSA; TOCSY, total correlation spectroscopy; ROESY, rotating-frame Overhauser effect spectroscopy; PPACK, D-Phe-Pro-Arg-chloromethylketone.

Table 1. *Sequences and numbering of divalent thrombin inhibitors and substrates*[a]

	Sequence																					
Inhibitor	1′	2′	3′	4′	5′	6′	7′	8′	53′	54′	55′	56′	57′	58′	59′	60′	61′	62′	63′	64′	65′	K_i
CVS995	PP-D	P	R-(COCO)	G	G	G	G	G	N	G	D	F	E	E	I	P	E		Y	L		1.0 pM
Hirugen									N	G	D	F	E	E	I	P	E	E	Y*	L		0.5 mM
Hirulog 1	dF	P	R-(CO)	G	G	G	G	G	N	G	D	F	E	E	I	P	E	E	Y	L		2.3 nM
Hirulog 3	dF	P	R-(CH_2CO)	G	G	G	G	G	N	G	D	F	E	E	I	P	E	E	Y	L		7.4 nM
Hirutonin 2	Ac-dF	P	R-($COCH_2$)	G	Q	S	H	N	N	G	D	F	E	E	I	P	E	E	Y	L	Q	0.3 nM
Hirutonin 6	Ac-dF	P	R-($COCH_2$)			Linker				G	D	F	E	P	I	P	L					3.5 nM
MDL28050											Suc-	Y	E	P	I	P	E	E	A	Cha-dE		29 nM[b]
Hirullin P18										S	D	F	E	E	F-S	L	D	D	I	E	Q	4.2 μM[b]
Thrombin platelet receptor	LD	P	R-S-F	L	L	R	N	P	N	D	K	Y	E	P	F	W	E	D	E	E		–

[a] Abbreviations: PP, 2-propylpentanoyl; all amino acids shown as single-letter codes; d, D-enantiomer; Ac, acetyl; linker, $(CH_2)_2$-$NHCH_2CO$-$CH{=}CH$-CH_2-$NHCH_2CO$-$CH{=}CH$-CH_2-; Suc, succinyl; Cha, cyclohexylalaninyl; Y*63′ in hirugen is sulfated tyrosine.
[b] IC_{50}.

a carboxy-terminal peptide resembling the FBS-binding segment of hirudin. The result of covalently linking a catalytic site moiety with an FBS-binding group gave inhibitors with significantly increased potency when compared to either of the individual components (active site tripeptide or FBS-binding peptide) alone. In addition, whereas the selectivity of the multivalent inhibitors was similar to that obtained with compounds that bound to the FBS alone, this parameter was improved dramatically over catalytic site-directed inhibitors (DiMaio et al., 1990; Maraganore et al., 1990). The residues containing the critical scissle bond range from proteolytically cleavable Arg-Pro (DiMaio et al., 1990; Maraganore et al., 1990) to stable pseudopeptide bonds (DiMaio et al., 1991, 1992; Kline et al., 1991; Qui et al., 1992).

Since Pauling first proposed the idea, it has been shown in several systems that functional groups that mimic the substrate transition state can be potent enzyme inhibitors. For serine proteases, such functionality includes aldehydes, trifluoromethyl ketones, and, more recently, α-keto-amides. A possible alternate form for a multi-valent inhibitor that would provide added molecular contacts with thrombin and possibly improve the overall affinity for the enzyme would incorporate an active site tripeptide with a transition-state mimetic that could mimic a stable, tetrahedral intermediate with Ser 195 of the catalytic triad. Many transition-state mimetics for serine proteases, e.g., aldehydes, trifluoromethyl ketones, are not amenable for this use because they do not allow extension into the P′ region toward the FBS. α-Keto-amides, however, do offer this unique capability of ready extension beyond the active carbonyl and into the P′ region. Analogues of these α-ketoamide transition-state inhibitors have been used to probe the importance of P′ residues in synthetic serine protease inhibitors (Powers & Harper, 1986). This functionality is also found in the naturally occurring thrombin inhibitor, cyclotheonamide (Fusetani et al., 1990; Hagihara & Schreibner, 1992; Lewis et al., 1993), in which the positioning of the α-keto-amide of cyclotheonamide within the catalytic center of thrombin has been shown to resemble the hemiketal tetrahedral intermediate, consistent with the transition state for peptide hydrolysis (Maryanoff et al., 1993).

We describe here the functional and structural characterization of several novel, multivalent inhibitors of thrombin that use an α-keto-amide transition-state mimetic bridging group to link a substrate-like active-site binding group with an FBS-binding peptide. In the most potent of these, CVS995 (Table 1), the P1–P3 residues of the amino-terminal functional group are derived from the thrombin recognition sites in the seven-transmembrane domain thrombin receptor (Vu et al., 1991a, 1991b) and protein C (Stenflo & Fernlund, 1982), and the FBS-binding carboxy-terminal segment is a variation of the carboxy-terminal region of hirudin. CVS995 is an extremely potent and selective inhibitor of thrombin amidolytic activity ($K_i = 1.01(\pm 0.32) \times 10^{-12}$ M) and is stable to proteolytic cleavage by α-thrombin. Analysis of the 2.3-Å resolution enzyme-bound structure reveals that the overall extent of interactions of CVS995 with thrombin resemble those reported for hirulog 3 (Qiu et al., 1992) and hirutonins 2 and 6 (Zdanov et al., 1993) (Table 1), but with the α-keto-amide bridging group forming a tetrahedral transition state with the active site serine and histidine residues in the catalytic triad. The potency and selectivity of CVS995 demonstrates the utility of the α-ketoamide transition-state mimetic as an uncleavable group that can be employed to link both catalytic and exosite-directed binding domains in inhibitors of serine proteases. A kinetic analysis of several bivalent peptides and their corresponding bivalent α-keto-amide counterparts shows that there is a complex and unexpected relationship between the contributions to binding energy due to the substrate sites, the transition-state analogue, and the FBS.

Results and discussion

Thrombin structure

The thrombin structure is well defined in the electron density (Table 2) except for a few terminal and autolysis loop residues (Ser 1E–Glu 1C, Ile 14K–Arg 15, Glu 247, Trp 148–Lys 149E (Kinemage 1)) that are consistently disordered in complexes of thrombin crystallizing in the space group C2 (Skrzypczak-Jankun et al., 1991; Qiu et al., 1992). The carbohydrate attached

Table 2. *Summary of final restrained least-squares parameters/deviations and R factor statistics of CVS995-thrombin structure*

	Target	RMS deviation
Distances (Å)		
Bond lengths	0.020	0.020
Angle lengths	0.035	0.050
Planar 1,4	0.050	0.055
Planes (Å)		
Peptides	0.023	0.020
Aromatic groups	0.023	0.020
Chiral volumes (Å^3)	0.15	0.20
Nonbonded contacts (Å)		
Single torsion	0.55	0.22
Multiple torsion	0.55	0.28
Possible H-bond	0.55	0.25
Torsion angles (degrees)		
Planar	3	3
Staggered	15	22
Orthonormal	20	30
Thermal parameters (Å^2)		
Main-chain bond	1.5	1.4
Main-chain angle	2.0	1.8
Side-chain bond	2.0	2.0
Side-chain angle	3.0	4.1

				R-value	
Dmin	Refs	$\langle\sigma(\lvert F_o\rvert)\rangle$[a]	$\langle\lvert\lvert F_o\rvert - \lvert F_c\rvert\rvert\rangle$[b]	Shell	Sphere
4.27	1980	32	87	0.159	0.159
3.53	1948	28	63	0.117	0.139
3.13	1921	25	56	0.144	0.140
2.86	1900	23	50	0.168	0.144
2.67	1797	21	41	0.157	0.146
2.52	1810	20	38	0.165	0.148
2.30	1666	18	35	0.166	0.149

[a] $\sigma(\lvert F\rvert) = 23.5 - 125.0(\sin\theta/\lambda - 1/6)$, applied as weight.
[b] Final $\langle\lvert\lvert F_o\rvert - \lvert F_c\rvert\rvert\rangle = 51.0$.

to Asn 60G could not be located in the electron density, and the overall solvent structure of the complex is similar to that of the other thrombin complexes.

CVS995 structure

Of the 20 residues in CVS995, PP to Ile 59′ were well defined in the electron density except for Gly 54′ (Fig. 1 and Kinemage 2). In addition, the carbonyl of the peptide bond between Gly 4′–Gly 5′ has two well-defined positions differing by about 45°; Gly 4′ was also anomalous in hirulog 3 (Qiu et al., 1992). The C-terminal four residues of CVS995 are disordered: the electron density maps using $(2\lvert F_o\rvert - \lvert F_c\rvert)$ and $(\lvert F_o\rvert - \lvert F_c\rvert)$ as coefficients at 0.8σ and 2σ levels, respectively, did not reveal any residues beyond Ile 59′. A similar disorder of the C-terminal 3_{10}-turn region of the hirudin peptide has also been found in the hirulog 1 complex (Skrzypczak-Jankun et al., 1991) (Table 1). However, when crystallized at a lower pH, in an orthorhombic space group, the 60′–64′ region of hirulog 1 and the autolysis loop of thrombin is ordered due to intermolecular packing interactions (Priestle et al., 1993). The same type of disorder also occurs in thrombin–aldehyde inhibitor–hirugen ternary complexes (Chirgadze et al., 1992; unpubl. results of A. Tulinsky laboratory). Variable binding behavior of the C-terminal segment has also been reported in other cases where the segment has different conformations (Qiu et al., 1993). Conversely, some or all of these residues are seen in a tetragonal ternary benzamidine thrombin complex (Banner & Hadvary, 1991) and the fibrinopeptide A–hirugen–thrombin complex (Stubbs et al., 1992).

A hydrophobic PP group is attached to the tripeptide sequence of Asp 1′-Pro 2′-Arg 3′ of CVS995 binding in the active site of thrombin, which is compared with that of PPACK in Figure 2. Noteworthy features of CVS995 are: (1) formation of a doubly hydrogen bonded ion pair in the S1 specificity site between the guanidinium group of Arg 3′ and Asp 189; (2) hydrophobic contacts with His 57, Tyr 60A, Trp 60D, and Leu 99 in S2 apolar site by Pro 2′; (3) hydrophobic interactions of the novel PP group with the S3 site; (4) formation of an antiparallel β-strand by the Asp 1′–Arg 3′ segment and Ser 214–Gly 216 of thrombin; and (5) the hydrogen bonding at the oxyanion hole of the carbonyl of Arg 3′ (Fig. 3; Table 3, Kinemage 2). The Arg 3′ side chain is additionally stabilized by hydrogen bonds NE-Ow 403, NH2-Ow 403, Ow 403-Phe 227O, and NH1-Gly 219O (Table 3). Furthermore, the carboxylate oxygen atoms of Asp 189 are similarly stabilized through a hydrogen bonding two-water molecule bridge (Ow 716, Ow 416) to Glu 217O and a single-water bridge (Ow 410) to Tyr 228OH (Table 3). Thus, the active site interactions follow a similar canonical binding mode exhibited by peptide substrates and inhibitors established previously by crystallography (Bode et al., 1989; Martin et al., 1992; Qiu et al., 1992; Stubbs et al., 1992). The conformation of the Pro 2′–Arg 3′ segment is essentially the same as that found in crystal structures of the other active site inhibitors of thrombin having this motif (Bode et al., 1989, 1992; Skrzypczak-Jankun et al., 1991; Priestle et al., 1993; Zdanov et al., 1993; Vijayalakshmi et al., 1994). The novel PP group makes 12 contacts < 4.0 Å with six different thrombin residues: Asn 98, Leu 99, Ile 174, Trp 215, Gly 216, and Glu 217 (Table 3); two of these (Leu 99, Ile 174) are usually associated with the aromatic S3 site that binds D-Phe in the PPACK–thrombin complex.

Acid residues at the P3 position of thrombin substrates are known to slow cleavage (Erhlich et al., 1990). However, thrombin becomes more efficient in cleaving such peptides when accompanied by binding at the FBS (e.g., in protein C/thrombomodulin [Esmon, 1989] and thrombin platelet receptor [Ishii et al., 1995]). This appears to be related to the conformation of Glu 192 in thrombin, which is in an extended conformation when the exosite is occupied and the P3 residue is acidic, thus distancing negative charge from the binding region (Vijayalakshmi at al., 1994). In the CVS995 complex, the situation is different because Glu 192 would collide with the Gly-linker when extended so that it is bent, as in the case where the active site is occupied by substrates lacking a negative charge at P3. In this conformation, Ow 423 mediates an interaction between Pro 2′O and Glu 192OE2 (Table 3). The carboxylate group of Asp 1′ interacts indirectly with Glu 192 via another water molecule (Ow 639) hydrogen bonding between Asp 1′OD2 and Ow 423, whereas Asp 1′OD1 hydrogen bonds directly to Gly 219N and indirectly to Arg 221ANH2 through Ow 451 (Table 3), similar

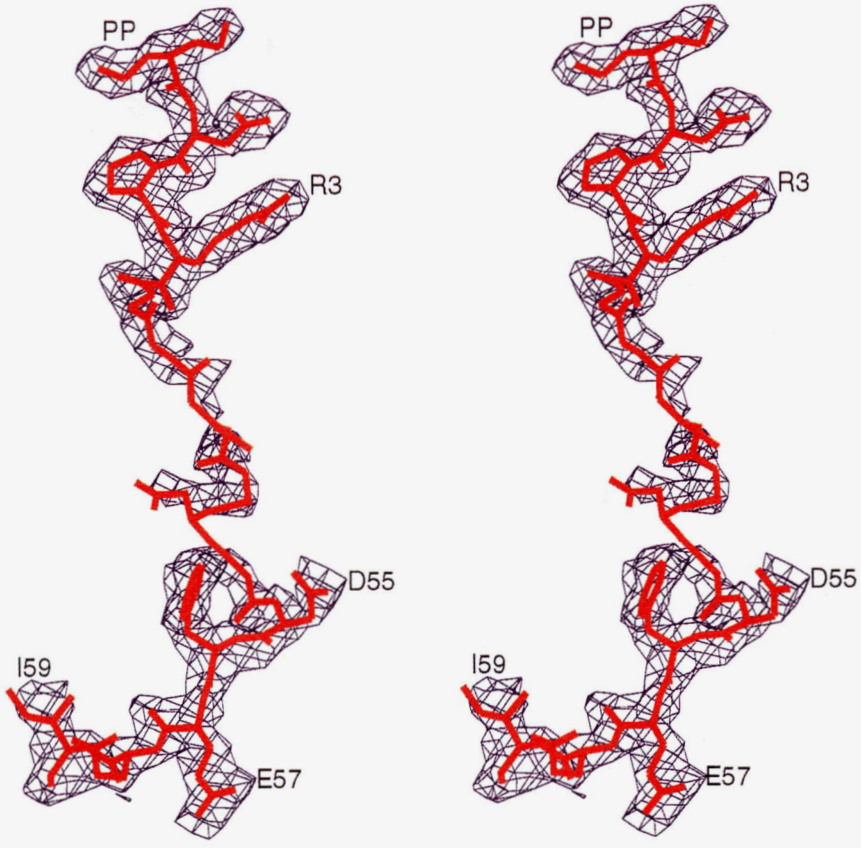

Fig. 1. Stereo view of the electron density for the divalent inhibitor CVS995 as it appears in its bound state with thrombin; basket contour level at 1σ; no density at Asn 53′, which is modeled.

to P3 of Leu-Asp-Pro-Arg of the thrombin platelet receptor (Mathews et al., 1994). This hydrogen bonding network fixes the P3 side-chain.

The α-keto-amide group, introduced to serve as a transition-state analogue of peptide hydrolysis, forms a tetrahedral intermediate and a network of hydrogen bonding interactions (Fig. 3 and Kinemage 2). The two carbonyl groups of the α-keto-amide group are oriented at a dihedral angle of 166°, akin to the carbonyls of cyclotheonamide and FK506 in the cyclotheonamide–thrombin (Maryanoff et al., 1993) and immunophilin FKBP–FK506 complexes (Van Duyne et al., 1991), respectively. The transition-state Arg 3′C–Ser 195OG bond is 1.74 Å, close to the 1.8 Å in the cyclotheonamide thrombin complex, but longer than the same bond in PPACK–thrombin (1.6 Å) (Bode et al., 1992) and the expected C-O single bond length of 1.45 Å. The OG oxygen impinges nearly orthogonally on the α-keto group (Arg 3′O-Arg 3′C-Ser 195OG = 102°, Arg 3′CA-Arg 3′C-Ser 195OG = 108°, and Arg 3′CA-Arg 3′C-Arg 3′O = 118°). The keto oxygen (Arg 3′O) makes hydrogen bonds with the amide nitrogen atoms of Gly 193 and Ser 195 of thrombin (Table 3); the former was observed in the transition-state intermediate of the phenylethane boronic acid chymotrypsin complex (2.7 Å) (Tulinsky & Blevins, 1987) and the latter was observed in PPACK–thrombin (Bode et al., 1989) (but longer at 3.1 Å). The oxygen atom of the amide group makes a good hydrogen bond with His 57 (2.7 Å), which utilizes the disrupted native geometrical arrangement between Ser 195 and His 57 (Vijayalakshmi et al., 1994). This hydrogen bond has been observed in the complex of thrombin with cyclotheonamide and also in the trypsin–cyclotheonamide complex (Lee et al., 1993). The Ser 195OG–His 57NE2 separation in unoccupied active-site thrombin complexes is about 3.0 Å (Vijayalakshmi et al., 1994), about 2.9 Å in the present complex and cyclotheonamide–thrombin, and 3.5 Å in the hirulog 3–thrombin complex, where His 57NE forms a hydrogen bond with Gly 4′N of the pentaglycine spacer. The distance between the carbon atom of the α-keto-amide and Ser 195OG is about 2.4 Å and about 3.5 Å from His 57NE2 compared to 2.1 Å and 1.9 Å of the covalent PPACK–thrombin complex, which most likely approximates posthydrolysis. These observations strongly suggest that the interaction of the α-keto group in the active site is that of a transition state of the thrombin scissile cleavage, where the substrate is undergoing catalysis but has not yet been cleaved.

In the thrombin complex, CVS995 has a generally extended conformation, but with bends at Gly 4′ and Asp 55′ (Figs. 1, 4). It spans the enzyme surface, displaying many interactions similar to hirulog 3 and hirutonin 2 at the active site and in the FBS. Although the overall interactions of CVS995 are similar to those of hirulog 3, the substitution of the methylene group of β-homoarginine residue in hirulog 3 by a carbonyl group in CVS995 makes subtle but significant changes in the hydrogen bonding pattern observed in the active site and S1′ subsite. The binding of Arg 3′ of CVS995 in the S1 specificity pocket is similar to the hirulog 1–thrombin complex rather than the β-homoArg 3′ of hirulog 3, where the CA atom of the residue is noticeably shifted and the side-chain conformation is in a less-favored

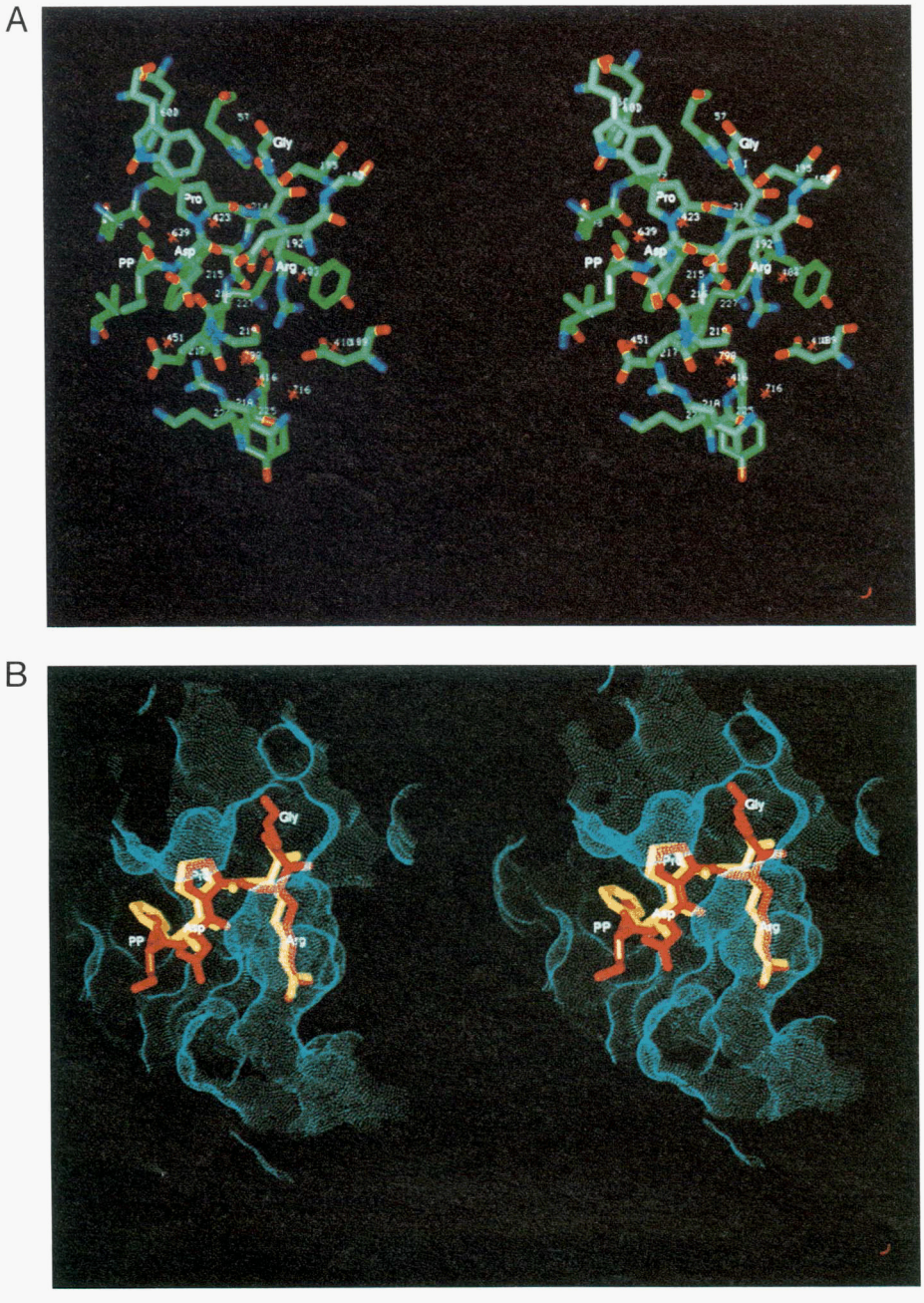

Fig. 2. A: Stereo view of the active site of CVS995–thrombin complex showing all interactions listed in Table 3. Thrombin residues are labeled by number and CVS995 residues are labeled by type. Atoms are colored by type (carbon, green; oxygen, red; nitrogen, blue). **B:** Stereo view of the superposition of CVS995 (red) and PPACK (yellow) in the solvent- (1.4 Å) accessible surface of the thrombin active site (blue dots) computed from the CVS995–thrombin complex.

rotomer state (Fig. 4). As a result, the change in χ-angle of Ser 195 from $-92°$ in hirulog 1–thrombin to $+28°$ in hirulog 3–thrombin is not observed in the CVS995 complex ($\chi = -90°$). Moreover, the oxygen atom of the arginyl amide group forms a hydrogen bond with His 57NE2 (Fig. 3). The carbonyl group of the first residue of the pentaglycine linker in CVS995 has two well-defined positions; thus, this residue does not form hydrogen bonds with Ser 195OG, Lys 60F and His 57NE2 as in hirulog 3 and the main-chain torsion angles of the first glycine (Gly 4′) fall in an allowed region, unlike Gly 4′ of the hirulog 3 complex ($\phi = 100°$, $\psi = -100°$).

Other carbonyl oxygen atoms of the main chain of the linker are only marginally defined in both CVS995 and hirulog 3. Therefore, caution was exercised in interpreting the electron density to place the glycine linker. Although the pentaglycine linker can be traced confidently, the exact position of each amide oxygen atom is not as certain as the main chain of the structure. Hence, some ambiguity exists, as in hirulog 3, in confirming the

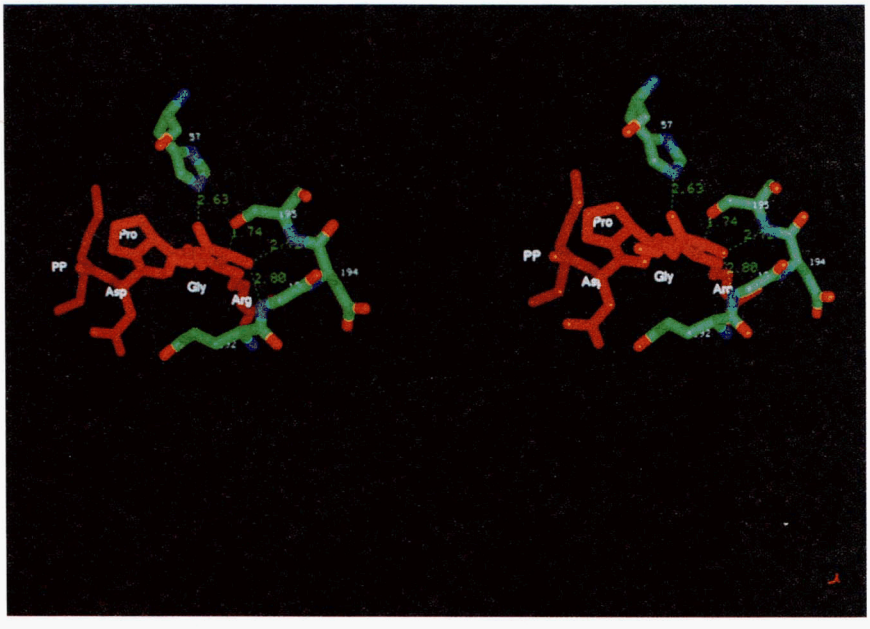

Fig. 3. Stereo view of interactions of the tetrahedral intermediate of CVS995 (red, labeled by residue type) with the oxyanion hole and the active site of thrombin (colored by atom type, residues labeled by number). Hydrogen bonds are shown with dotted lines with heavy atom distances.

S2′–S4′ subsites exactly. The pentaglycine linker interactions of CVS995 are compared with hirulog 3–thrombin associations in Table 4. The somewhat different interactions of the glycine linker result from the hydrogen bond organization in and around the active site because of the α-keto-amide group.

The main-chain structure of the Asn 53′ to Ile 59′ segment is similar to that observed in hirudin, hirugen, hirulogs 1 and 3, hirutonins 2 and 6, hirullin P18 and MDL 28050 (Qiu et al., 1993), and the comparable segment of thrombin platelet receptor peptide (Mathews et al., 1994) (Table 1). Noteworthy interactions are: (1) the formation of a hydrogen bonded salt bridge between Asp 55′ and Arg 73, and (2) hydrophobic contacts between Phe 56′, Ile 59′, and Phe 34, Gln 38, Leu 65, Ile 82, and Tyr 76. The interaction between Glu 57′ and a crystallographically related molecule is ambiguous because neighboring Arg 75 side-chain atoms do not have complete density. The structure of the region, however, is very similar to the intermolecular salt bridge formed by these two residues in the hirugen–thrombin and hirudin–thrombin crystal structures. The side-chain atoms of Glu 58′ residue have no electron density, as in hirulogs 1 and 3, and hirutonin 2 and hirullin P18, whereas in hirutonin 6, MDL28050, and the platelet receptor peptide, they are a well-defined proline residue. This same Glu 58′ residue, however, was found to be ordered and interacting with a symmetry-related thrombin molecule (Arg 93) in the lower pH thrombin complexes crystallizing in an orthorhombic space group (unpubl. results of A. Tulinsky laboratory), and not with Arg 77A, the β cleavage site of thrombin, as in the hirudin–thrombin complex. As described elsewhere (Qiu et al., 1992), the protection against β cleavage at Arg 77A by hirugen and hirulog 3 is more by physical obstruction rather than specific interactions at the autolytic cleavage site. The same applies to CVS995.

The lack of a bound structure for Pro 60′–Leu 64′ of CVS995 is similar to the behavior of hirulog 1, where cleavage occurred at the scissile bond in the active site, additionally resulting in a linker peptide that was disordered. A likely cause of the lack of stable structure of the C-terminal segment of CVS995 could be due to an inability to conformationally adjust to the 3_{10}-turn hydrophobic binding patch on the thrombin surface, as has been observed in hirullin P18 and MD28050 complexes of thrombin (Qiu et al., 1993). This, in turn, could be related to the different terminal peptide sequence of CVS995 (missing Glu 62′). The response of this part of FBS peptides has been generally variable and even anomalous in the instance of hirulog 1 and hirulog 3, where the former is disordered and the latter is not. The deletion relative to the hirugen sequence occurs adjacent to the critical Tyr 63′ residue and likely causes its dislocation. Interestingly, Tyr 63′ was previously thought to be important because its mutation to Ala in hirudin resulted in a loss of 2.2 kJ/mol in binding energy, possibly due to the loss of hydrophobic contact with thrombin residue Ile 82. The deletion of Glu 62′ apparently does not permit high occupancy of Leu 64′ in the site normally filled by Tyr 63′. This is consistent with the Tyr 63′Leu mutant of hirudin showing a 3.1 kJ/mol loss in binding energy relative to the native inhibitor (Betz et al., 1991). Thus, it is not surprising that the C-terminal residues of CVS995 do not show well-ordered structure with the thrombin FBS.

The interactions of CVS995, hirutonin 2, and hirutonin 6 correspond closely to those observed with the hirulog 3–thrombin and hirudin–thrombin complexes (Qiu et al., 1992). Superposition of CVS995, hirulog 3, and hirutonin 2 shows that these inhibitors have a similar overall structure (Fig. 4). The main chain of the pentaglycine linker of CVS995 makes a much closer contact with thrombin (as does hirulog 3) compared to Lys 47′–

Table 3. *Important interactions of CVS995 in the active site of thrombin*

Interacting atoms[a]		Distance (Å ± 0.25)
PP CD1	Asn 98 CA	3.8
PP CD1	Asn 98 C	3.7
PP CD1	Asn 98 O	3.8
PP CD1	Leu 99 CD2	3.9
PP CB1	Ile 174 CD1	3.9
PP CD1	Trp 215 CD2	3.9
PP CB1	Trp 215 CE3	3.8
PP CG1	Trp 215 CD2	4.0
PP CB2	Gly 216 O	4.0
PP CG2	Gly 216 O	3.9
PP CB2	Glu 217 OE1	3.1
PP CG2	Glu 217 OE1	3.3
Asp 1′ N	Gly 216 O	2.6
Asp 1′ O	Gly 216 N	3.0
Asp 1′ OD1	Gly 219 N	2.8
Asp 1′ OD1	Ow 451	3.2
Asp 1′ OD2	Ow 639(Ow 423)	2.6 (2.9)
Pro 2′ CB	His 57 CD2	3.8
Pro 2′ CB	His 57 NE2	3.8
Pro 2′ CB	Leu 99 CD2	3.9
Pro 2′ CG	Tyr 60A CE2	3.8
Pro 2′ CG	Tyr 60A CZ	3.8
Pro 2′ CG	Tyr 60A OH	3.8
Pro 2′ CG	Trp 60D CH2	3.8
Pro 2′ O	Ow 423(Glu 192 OE2)	2.9 (3.0)
Pro 2′ O	Glu 192 CG	3.6
Arg 3′ C	Ser 195 OG	1.7
Arg 3′ O	Ser 195 N	2.7
Arg 3′ O	Gly 193 N	2.8
Arg 3′ N	Ser 214 O	3.3
Arg 3′ NH1	Asp 189 OD	2.8
Arg 3′ NH2	Asp 189 OD2	2.7
Arg 3′ NH1	Gly 219 O	2.8
Arg 3′ NE	Ow 820(Glu 192 OE2)	3.0 (2.5)
Arg 3′ NH2	Ow 403(Phe 227 O)	3.0 (2.7)
COCO′ O	His 57 NE2	2.6
Asp 189 OD1	Ow 716(Ow 416,Asp 221 N)	2.7 (2.8,2.9)
Asp 189 OD2	Ow 410(Tyr 228 OH)	2.8 (3.0)
Glu 217 N	Ow 798(Tyr 225 O)	3.1 (2.9)
Gly 219 O	Ow 820	2.6
Arg A N	Ow 416(Ow 798)	3.1 (2.6)
Arg 221A NH2	Ow 451	2.6
Arg 221A NH1	Ow 451	3.3
Lys 224 O	Ow 409(Ow 716)	2.4 (3.1)
Phe 227 O	Ow 403	3.1

[a] Parenthetical atoms and distances denote extended stes of hydrogen bonds.

Gly 54′ of the natural inhibitor hirudin. The Glu 192 residue is well defined in electron density and interacts through water molecule Ow 423 with the carbonyl oxygen of Pro 2′ and with Asp 3′ through an additional water molecule (Ow 423 and Ow 639). Its compact orientation, however, is typical for active-site-occupied thrombin, where the substrate does not possess a negative charge at the P3 subsite (Vijayalakshmi et al., 1994). A critical role for the position of Glu 192 is suggested in protein C activation by the thrombomodulin–thrombin complex, which displays sensitivity to the substrate sequence at P3 (Le Bonniec & Esmon, 1991). In CVS995, Glu 192 cannot assume an extended conformation because it would then collide with the Gly-linker on the S1′-S2′ region of the extended binding site. Whether the same occurs with substrates like protein C and thrombin platelet receptor remains to be determined.

Table 4. *Pentaglycine spacer[a] interactions with thrombin*

Interacting atoms		Distance (Å) CVS995	Hirulog 3
Gly 4′ N	Ser 195 OG	3.8	3.1
Gly 4′ CA	Leu 41 O	3.8	–
Gly 4′ O	Lys 60F NZ	3.8	–
Gly 5′ O	Gly 193 N	3.7	3.2
Gly 6′ N	Leu 40 O	3.2	3.5
Gly 7′ O	Leu 40 N	3.5	2.6
Gly 7′ O	Glu 39 OE2	3.4	3.6
Gly 8′ O	Gln 151 NE2	3.7	–

[a] Gly 7′ and Gly 8′ are modeled positions.

Thrombin inhibition

The structural conservation of the 53′ to 59′ segments for hirulog 1, hirulog 3, hirugen, and CVS995 suggests that there is a general similarity of exosite binding notwithstanding differences in the active-site region or deletions in the extreme C-terminus. It might be expected that the deletion of Glu 62′ in CVS995 and the concomitant dislocation of Tyr 63′ and Leu 64′ would lead to poorer inhibitors of thrombin. In fact, for peptide inhibitors with the Arg-Pro scissile bond, this is exactly what is observed when the binding constants of inhibitors **3** versus **4** and inhibitors **2** versus **5** in Table 5 are examined. In these cases, the deletion causes a 5–7-fold reduction in binding affinity. Surprisingly, although the deletion results in crystallographic disorder in CVS995 and possible loss of specific binding, the C-terminus of the Glu 62′ deletion mutant still contributes significantly to the binding affinity, because its removal in compound **6** leads to a greater than 40-fold reduction in affinity for the divalent peptide (Table 5). The effect of the C-terminal truncation in these peptides is about the same as that observed for the truncation of hirudin (Skrzypczak-Jankun et al., 1991). Although the deletion reduces peptide activity, it is, in dramatic contrast, quite beneficial for the divalent α-keto-amide inhibitor CVS995, which is 26-fold *more* potent than compound **8** that contains the full native C-terminal sequence.

For the case of intact hirugen-like exosite fragments, replacing the Arg-Pro cleavable bond with the Arg-(CO)-Gly group leads to a 200–300-fold improvement in K_i (compare **1** with **7** or **2** with **8** in Table 5). If the interactions between thrombin and the active site and FBS segments of the inhibitors were additive, one would expect to see a 200–300-fold improvement in the other α-keto-amide inhibitors. Additionally, one would expect to see the affinity of the Glu 62′-deleted and the C-terminal-truncated keto-amides to be reduced about 5–7-fold and 300-fold, respectively, compared to the native-like inhibitor.

Surprisingly, the deletion α-keto-amide (CVS995) is 26-fold more potent than the native-like α-keto-amide inhibitor **8** and

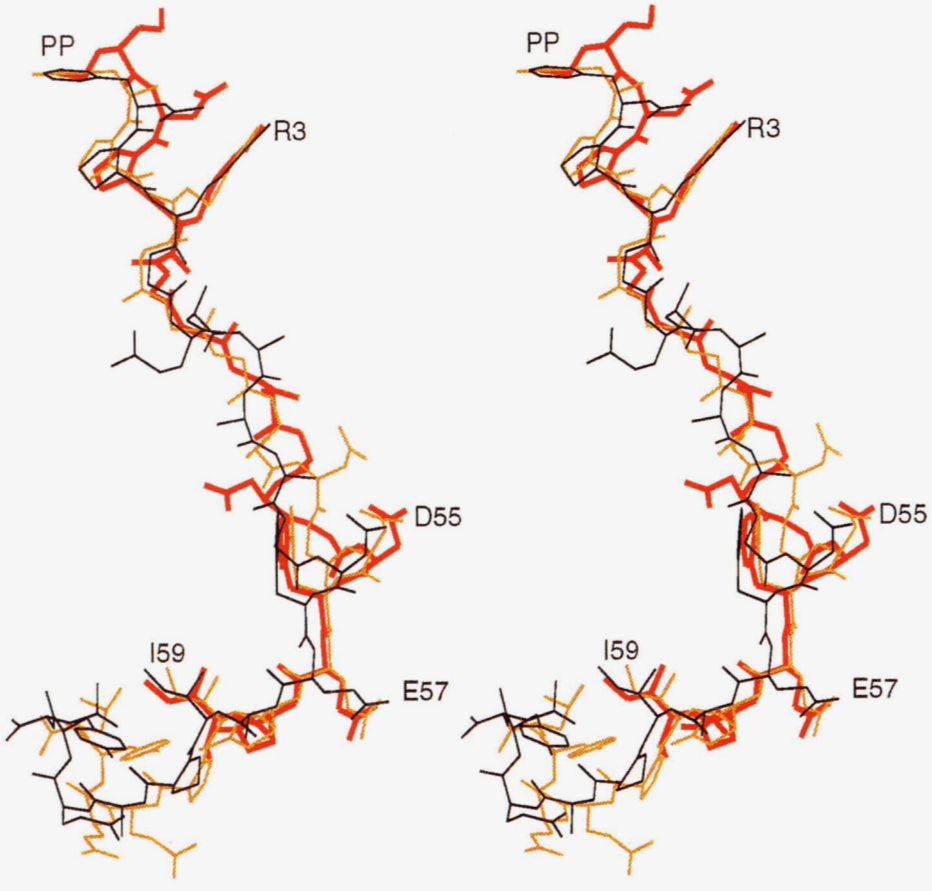

Fig. 4. Stereo view of the superposition of CVS995 (red), hirulog 3 (yellow), and hirutonin 2 (black) showing their overall similarity when bound to thrombin. Gly 54′ of CVS995 and Gly 8′, Asn 53′, and Gly 54′ of hirulog 3 modeled.

truncated α-keto-amide **9** is about equipotent to **8**. Viewed in terms of the effect of the Arg-(CO)-Gly replacement for Arg-Pro, the α-keto-amide in the Glu 62′-deleted inhibitor (CVS995) improved activity by 58,000-fold over its peptide counterpart **5**, and the C-terminal-truncated α-keto-amide improved activity by 83,000-fold over its peptide counterpart **6**. Both of these activity improvements are strikingly greater than the 200–300-fold improvements seen for the native sequence. It is clear that the interaction energies of the active-site, transition-state, and exosite regions of these inhibitors are not additive! The transition-state binding of the α-keto-amide group gives the largest binding energy increase to the bivalent peptide with the lowest binding energy of the set examined. The effect of this unusual property of the α-keto-amide group is that the best divalent keto-amide inhibitor is derived from a moderate divalent peptide inhibitor, and the activity range of the keto-amide inhibitors is compressed relative to the range of the peptides.

At present, the current structure has not suggested the reason for the dramatic nonadditivity of binding components of the transition state with the active site and exosite. The cause

Table 5. *Binding constants of selected divalent peptide and α-keto-amide thrombin inhibitors*

	Divalent peptide[a]	K_i (nM)		Divalent α-keto-amide[a]	K_i (nM)	Ratio
1	Ac-dPhe-Pro-Arg-Pro-$(Gly)_4$-*A*	10.0	**7**	Ac-dPhe-Pro-Arg-(CO)-Gly-$(Gly)_4$-*A*	0.046	220
2	PP-Asp-Pro-Arg-Pro-$(Gly)_4$-*A*	7.7	**8**	PP- Asp-Pro-Arg-(CO)-Gly-$(Gly)_4$-*A*	0.026	300
3	H-dPhe-Pro-Arg-Pro-$(Gly)_4$-*A*	0.69				
4	H-dPhe-Pro-Arg-Pro-$(Gly)_4$-*B*	3.4				
5	PP-Asp-Pro-Arg-Pro-$(Gly)_4$-*B*	58.0	**CVS995**	PP- Asp-Pro-Arg-(CO)-Gly-$(Gly)_4$-*B*	0.001	58,000
6	PP-Asp-Pro-Arg-Pro-$(Gly)_4$-*C*	2500.0	**9**	PP- Asp-Pro-Arg-(CO)-Gly-$(Gly)_4$-*C*	0.030	83,000

[a] *A* = Asn-Gly-Asp-Phe-Glu-Glu-Ile-Pro-Glu-Glu-Tyr-Leu; *B* = Asn-Gly-Asp-Phe-Glu-Glu-Ile-Pro-Glu-Tyr-Leu; *C* = Asn-Gly-Asp-Phe-Glu-Glu-Ile.

of this unusual behavior for the α-keto-amides does not appear to be related to solution structure because there was very little NMR evidence for any such structure. It is likely that the explanation will be found in the dynamics of binding and/or the kinetic mechanism. These possibilities are currently under investigation. It is interesting and perhaps sobering for rational drug design efforts to find that kinetically significant effects can be derived from a portion of an inhibitor that may show no ordered structure in its complex.

Materials and methods

Synthesis

CVS995

Starting with Boc-Leu-Pam Resin (Advanced ChemTech, Louisville, Kentucky), N-α-t-Boc amino acids were coupled successively on an Applied Biosystems 430A Peptide Synthesizer using the standard protocols of ABI (Users Manual, Part No. 901889, Rev. B, Version 2, Jan. 1992). Deblocking of the N-α-t-Boc group with TFA was followed by neutralization with diisopropylethylamine and coupling of the next N-α-t-Boc amino acid using 1-hydroxybenzotriazole hydrate and benzotriazole-1-yloxy-tris(dimethylamino)-phosphonium hexafluorophosphate . The coupling efficiency was monitored by the Kaiser ninhydrin test. N-α-t-Boc-O-(2-bromobenzyloxycarbonyl)-L-tyrosine was coupled to the Leu-Pam resin followed by N-α-t-Boc-L-glutamic acid-γ-cyclohexyl ester, N-α-t-Boc-L-proline, N-α-t-Boc-L-isoleucine, N-α-t-Boc-L-glutamic acid-γ-cyclohexyl ester, N-α-t-Boc-L-glutamic acid-γ-cyclohexyl ester, N-α-t-Boc-L-phenylalanine, N-α-t-Boc-L-aspartic acid-β-cyclohexyl ester, N-α-t-Boc-glycine, N-α-t-Boc-N-d-xanthyl-L-asparagine, five cycles of N-α-t-Boc-glycine, 6-nitroguanidino-3-(*S*)-t-Boc-amido-2-(*R,S*)-hydroxy-hexanoic acid, N-α-t-Boc-L-proline, and N-α-t-Boc-L-aspartic acid-β-cyclohexyl ester. In the final coupling cycle, 2-propylpentanoic acid was coupled in the same manner as the N-α-t-Boc amino acids. The resin-bound hydroxyamide peptide was oxidized to the α-keto-amide by treatment of the suspended resin-peptide with dimethylsulfoxide followed by 1-(3-dimethylaminopropyl)-3-ethylcarbodiimide hydrochloride in DCM. Dichloroacetic acid was added while maintaining the reaction temperature at 20–25 °C. After 1 h, the resin was filtered and washed with DCM and ether. A small portion of the resin was removed and cleaved with HF. The efficiency of the oxidation was checked by HPLC (Vydac C-18 25cm × 4.6 cm column, 20 min 20–35% acetonitrile/water gradient [0.1% TFA], 1 mL/min flow rate) where the desired product had a retention time of ~23 min. When the oxidation was complete, the bulk of the product was deprotected and cleaved from the resin with HF at −20 °C followed by slow warming to 10 °C. After evaporation of the HF under a stream of nitrogen, the peptide was extracted into 20% aqueous acetic acid and purified by HPLC on a Waters Delta-Prep 4000 with a Vydac C-18 column (50 × 250 mm, particle size 15–20 μm). An acetonitrile/water (0.1% TFA) gradient was used with a flow rate of 125 mL/min. An overall yield of 11% was obtained of lyophilized, purified material. The final product was characterized by FAB mass spectroscopy (M+H 2134) and analytical HPLC (97% purity) with the same analytical conditions as used for monitoring the oxidation. Amino acid analysis of the lyophilized powder gave a peptide content of 76%.

6-nitroguanidino-3-(S)-t-Boc-amido-2-(R,S)-hydroxy-hexanoic acid

A mixture of N-α-t-Boc-L-nitroarginine in THF was cooled under nitrogen to −5 °C, neutralized with an equimolar amount of *N*-methylpiperidine, and reacted with isobutylchloroformate to form the mixed anhydride. In a separate flask, an equimolar amount of *N*-methyl-*O*-methyl-hydroxylamine hydrochloride in DCM was cooled to 0 °C and neutralized with an equimolar amount of *N*-methylpiperidine. The free base *N*-methyl-*O*-methyl-hydroxylamine was added slowly to the mixed anhydride and the reaction mixture was stirred for 1.5 h at −5 °C, at which time the reaction to form the *N,N*-methoxy-methyl amide of N-α-t-Boc-L-nitroarginine was complete (thin layer chromatography 1:10:90 acetic acid:methanol:DCM). The reaction mixture was filtered and the filtrate was concentrated in vacuo. The product was dissolved in DCM and flash chromatographed on a silica gel column (DCM, followed by 2% methanol in DCM, followed by 5% methanol in DCM). Fractions containing pure product were pooled and concentrated in vacuo to give carboxamide in 88% yield. Residual methanol and traces of water were removed by redissolving the product in 50:50 (v/v) DCM:toluene and concentrating again in vacuo. The product was dissolved in dry THF and cooled to −70 °C. An equimolar amount of lithium aluminum hydride in THF and a 0.1 equivalent amount of diisobutyl aluminum hydride in hexane was added to the cooled arginine amide. The mixture was stirred at −70 °C for 0.5 h and slowly warmed to 0 °C over about 2 h. The reaction mixture was again cooled to −70 °C and quenched with 2 M potassium bisulfate. The mixture was allowed to warm to 0 °C and the precipitated salts were filtered and washed with THF. The combined filtrate/washes were concentrated in vacuo until most of the THF was removed, leaving the product and residual water. This hydrated product was dissolved in ethyl acetate and washed (with appropriate back washes) sequentially with 2 M hydrochloric acid and sodium bicarbonate. The combined organic fractions were dried and concentrated in vacuo to give an 88% yield of N-α-t-Boc-L-nitroargininal. The cyanohydrin of the protected argininal was prepared by the addition of a 5 M excess of potassium cyanide and 16 M excess of potassium bicarbonate in water to the argininal dissolved in THF. The organic phase was separated and the water phase was washed (with appropriate back washes) with ethyl acetate. The combined organic fractions were dried and concentrated in vacuo to give the cyanohydrin as a white solid (100% yield). This intermediate was treated with anhydrous, hydrochloric acid-saturated methanol, which removed the Boc group and converted the cyano group to a methyl imidate. The imidate was subsequently converted to a mixture of methyl ester and carboxylic acid upon the addition of 6 M HCl. The solution was concentrated in vacuo and taken up in methanol. The solution was once again concentrated in vacuo and the resulting foam was dissolved in anhydrous methanol. The solution was saturated with HCl to convert any carboxylic acid present to methyl ester. The volatiles were removed in vacuo, the crude product taken up in methanol, and this solution added to a biphasic mixture of saturated aqueous sodium bicarbonate and THF containing 1.5 equivalents of di-*t*-butyldicarbonate. After prolonged stirring, the mixture became bi-

phasic again and the organic phase and the ethyl acetate washes of the aqueous phase were combined, washed, dried, and concentrated in vacuo. The crude product was purified with silica gel flash chromatography (1% methanol in DCM up to 5% methanol in DCM) and pure fractions were concentrated in vacuo to yield 56% of pure hydroxy ester. The final product, 6-nitroguanidino-3-(*S*)-t-Boc-amido-2-(*R,S*)-hydroxy-hexanoic acid, was prepared by lithium hydroxide hydrolysis of the hydroxy ester to yield free acid in quantitative yield.

Other α-keto-amides

Compounds **7**, **8**, and **9** of Table 5 were all prepared in a manner analogous to that of CVS995. Each compound was characterized by HPLC and mass spectroscopy.

Peptides **1–6**

All peptides shown in Table 5 were prepared by conventional Boc peptide synthesis chemistry (as summarized above for CVS995) and characterized by HPLC and mass spectroscopy.

Crystallization

The thrombin–CVS995 complex was made by placing about a 10-fold molar excess of solid CVS995 over a frozen 1.0-mL sample of α-thrombin (0.81 mg/mL in 0.75M NaCl). This was then diluted to 2.0 mL with 0.1 M sodium phosphate buffer, pH 7.3, and the solution was concentrated to about 3.5 mg/mL. Crystals were grown from 8 μL hanging drops with 1.8 mg/mL protein complex, 0.075 M sodium phosphate buffer, pH 7.3, 0.19 M NaCl, 12% PEG 8000, equilibrating against well solutions of 0.1 M sodium phosphate buffer, pH 7.3, 24% PEG 8000. A crystal measuring 0.45 × 0.30 × 0.15 mm was used for the X-ray measurements.

Intensity data collection

The crystals were characterized and X-ray diffraction data were collected using a Siemens multiwire X-1000 area detector mounted on a Siemens P3/F four-circle goniostat. Graphite monochromated Cu K_α radiation was generated by a Rigaku RU200 rotating anode source at 7.5 kW power (50 kV, 150 mA) collimated to 0.3 mm. The crystal-to-detector distance was set at 11.65 cm. The detector swing angle was −15°, the scan range was 0.2° per frame and each frame was collected for 90 s. The program XENGEN (Howard et al., 1987) was used to process the raw data to obtain integrated intensities. The crystal diffracted X-rays to 2.3 Å resolution with the average peak width of 0.6° and was isomorphous with the hirugen, hirulog 1, hirulog 3 complexes (Table 1) and other ternary complexes (with active site inhibitors and hirugen at the exosite) of thrombin (Skrzypczak-Jankun et al., 1991; Qiu et al., 1992): monoclinic, space group C2, four molecules per unit cell with $a = 70.88$ Å, $b = 72.21$ Å, $c = 73.22$ Å, and $\beta = 100.9°$ ($V_m = 2.4$ Å/Da, protein fraction 51%). After XENGEN data reduction, a total of 14,238 independent measurements were obtained from 47,817 collected measurements. Removing weak data with $I/\sigma(I) \leq 2$ produced a data set of 13,616 unique reflections (75% observed, $R_{merge} = 0.061$). This data set is complete to 2.5 Å resolution and has half of the possible reflections between 2.5 Å and 2.3 Å resolution.

Structure determination and refinement

The phases of the CVS995 complex were approximated using the thrombin coordinates of the thrombin–hirugen complex (Brookhaven Protein Data Bank accession number 1HGT). The structure was refined using restrained least-squares methods with the program PROLSQ (Hendrickson, 1985). The starting model included residues Ser 1E–Arg 15 of the A chain, Ile 16–Leu 144 and Gln 151–Glu 247 of the B chain (chymotrypsinogen numbering [Bode et al., 1989]). The initial crystallographic *R*-factor ($R = \Sigma(\|F_o| - |F_c\|)/\Sigma|F_o|$) was 0.34 and reduced to 0.22 after 15 cycles of refinement. The first $2(|F_o| - |F_c|)$electron density from (7.0–2.8) Å resolution showed density for most of the thrombin residues, residues PP and the arginyl α-keto-amide in the active site, and Asp 55′–Ile 59′ in the exosite; all were also prominent in the $(|F_c| - |F_o|)$ difference map. However, as in other complexes, there was no density for Trp 148–Lys 149E of the autolysis loop of thrombin as in other isomorphous thrombin complexes. This new model was improved further by fitting the electron density on an Evans & Sutherland PS390 stereographics system with the program FRODO (Jones, 1982).

The dictionary file was modified to introduce proper restraints to the PP residue and the α-keto-amide group. The "transition-state" hemiketal target structure was taken to be the calculated structure and refined with more relaxed restraints (0.05–0.07 Å). This target structure was periodically updated during refinement with the latest calculated structure of the hemiketal. The PROLSQ refinement proceeded by a series of geometrically "tight-loose-tight" restrained cycles, starting with an overall thermal parameter of 30 Å^2 at 2.8 Å resolution, then proceeding to individual thermal parameters and gradually increasing resolution (to 2.5 and then to 2.3 Å); water molecules were introduced at 2.5 Å resolution. The final structure converged at $R = 0.149$ with an average thermal parameter of 26 Å^2 using 167 water molecules with occupancy greater than 0.5 and 13,022 reflections from 7.0 to 2.3 Å resolution.

In the final stages, reflection weight option of PROLSQ that was Bragg angle-dependent replaced constant weights (Hendrickson, 1985), which were assigned based on $\langle \|F_o| - |F_c\| \rangle/2$ in various angle ranges. The final *R* values in different ranges are given in Table 2, along with a summary of refinement parameters.

The ω angles of 97% of the peptide bonds of the thrombin part of the structure are within ±6° of planarity and the distribution of main-chain torsion angles of the complex shows that all the non-glycine amino acids fall within or close to the allowed regions in the Ramachandran map. The coordinates of the final structure have been deposited in the Brookhaven Protein Data Bank [access number 1DIT].

Binding constant (K_i) determination

Human thrombin was purchased from Enzyme Research Laboratories, Inc. (South Bend, Indiana); its concentration was predetermined by the supplier from the absorbance at 280 nm, and the extinction coefficient. The activity of this material was 3,806 NIH units/mg. The chromogenic substrate Pefachrome tPA (CH_3SO_2-D-hexahydotyrosine-glycyl-arginine-*p*-nitroanaline·

AcOH, Pentapharm, Ltd, Basel, Switzerland) was obtained from Centerchem, Inc. (Tarrytown, New York). The substrate was reconstituted in ultrapure water prior to use. The enzymatic reactions were monitored in the wells of a microtiter plate by measuring the increase in absorbance at 405 nm, using a Thermomax microplate reader (Molecular Devices, Menlo Park, California); this change in absorbance directly reflected thrombin's cleavage of Pefachrome tPA and the release of *p*-nitroaniline. Inhibitors were diluted into HBSA, 10 mM HEPES, 150 mM NaCl, and BSA, 0.1% (w/v), pH 7.5. To individual wells, either 100 μL of inhibitor, or, in the case of the uninhibited control, 100 μL of HBSA, were combined with 100 μL of Pefachrome tPA. Reactions were initiated by the addition of 50 μL of human thrombin. All reactions were performed in triplicate in a final volume of 250 μL of HBSA, containing, at final concentration: 250 pM thrombin, 400 μM Pefachrome tPA, and, depending on the inhibitor, 0.1–1.2 nM for the α-keto-amide inhibitors, 0.001–25 μM for all peptides, with the exception of 0.1–250 μM for **6** (Table 5). The inhibition reactions were measured for either 30 min at 15-s intervals for the α-keto-amide inhibitors, or 5 min at 9-s intervals for all peptides at ambient temperature under steady-state conditions, where less than 5% of the substrate was consumed.

Kinetic constants describing the inhibitory interaction of α-keto-amide inhibitors with thrombin were calculated from generated progress curves, reflecting the slow inhibition by the ketoamide inhibitors of thrombin. Data representing each progress curve were fit directly by nonlinear regression to the integrated first-order rate Equation 1, described by Cha (1975) and Williams and Morrison (1979), shown below.

$$P = V_s t + (V_0 - V_s)(1 - e^{-k_{obs}t})/k_{obs}, \quad (1)$$

where V_0 is the initial uninhibited velocity, V_s is the final steady-state inhibited velocity, and k_{obs} is the apparent first-order rate constant, which describes the equilibration of the inhibitory reaction from the initial to the final steady state. The inhibition of thrombin by CVS995 can then be described by Equation 2, which relates the measured values of k_{obs} over a range of inhibitor concentrations to calculated rate constants (Morrison, 1982).

$$k_{obs} = k_1[I]/(1 + [S]/K_m) + k_{-1}, \quad (2)$$

where k_1 is the second-order association rate constant describing the formation of the enzyme–inhibitor complex, k_{-1} is the dissociation rate constant. The equilibrium dissociation rate constant K_i is calculated from a ratio of k_1 to k_{-1}. Because the inhibition of thrombin by peptides was rapidly achieved, velocity data could be plotted directly against the inhibitor concentration, and then fit to a curve described by the 4-parameter Equation 3, giving term C:

$$Y = (A - D)/(1 + (X/C)^B) + D. \quad (3)$$

K_i was calculated from term C of Equation 3 using Equation 4.

$$K_i(1 + [S]/K_m) = C. \quad (4)$$

Nuclear magnetic resonance experiments

CVS995 was dissolved in 10% D_2O/90% H_2O to a concentration of 1 mM with an ambient pH of 2.7. Conventional 2D TOCSY and ROESY experiments were performed at 25 °C with a Varian-Unity 600 MHz spectrometer. Spin system assignments were determined for all amino acids, and sequential assignments were determined for all but the glycine linker residues. Only two weak long-range ROESY crosspeaks were observed, implying that CVS995 has little stable tertiary structure in water.

Acknowledgments

We thank Dr. Thomas Webb for beneficial synthesis discussions, Michael Weinhouse and Steven Carpenter for synthesis assistance, Dr. Klaas Hallenga for NMR support, and Dr. K.P. Padmanabhan for growing the crystals of the CVS995–thrombin complex. Part of this work was supported by NIH grant HL43229 (A.T.).

References

Banner DW, Hadvary P. 1991. Crystallographic analysis at 3.0 Å resolution of the binding to human thrombin of four active site-directed inhibitors. *J Biol Chem 266*:20085–20090.

Betz A, Hofsteenge J, Stone SR. 1991. Role of interactions involving C-terminal nonpolar residues of hirudin in the formation of the thrombin–hirudin complex. *Biochemistry 30*:9848–9853.

Bode W, Mayr I, Baumann U, Huber R, Stone SR, Hofsteenge J. 1989. The refined 1.9 Å crystal structure of human α-thrombin: Interaction with D-Phe-Pro-Arg chloromethyl ketone and significance of the Tyr-Pro-Pro-Trp insertion segment. *EMBO J 8*:3467–3475.

Bode W, Turk D, Karshikov A. 1992. The refined 1.9 Å X-ray crystal structure of D-Phe-Pro-Arg chloromethylketone-inhibited human α-thrombin. Structure analysis, overall structure, electrostatic properties, detailed active-site geometry, structure–function relationships. *Protein Sci 1*: 426–471.

Cha S. 1975. Tight-binding inhibitors. I. Kinetic behavior. *Biochem Pharmacol 24*:2177–2185.

Chirgadze NY, Clawson DK, Gesellchen PD, Hermann RB, Kaiser RE Jr., Olkowski JL, Sall DJ, Schevitz RW, Smith GF, Shuman RT, Wery JP, Jones ND. 1992. The X-ray structure at 2.2 Å resolution of a ternary complex containing human α-thrombin, a hirudin peptide (54–65) and an active site inhibitor. Pittsburgh, Pennsylvania: ACA Annual Meeting, August 9–14. Abstract PB33.

Coughlin SR. 1994. Thrombin receptor function and cardiovascular disease. *Trends Cardiovasc Med 4*:77–83.

DiMaio J, Gibbs B, Lefebre J, Konishi Y, Munn D, Yue SY. 1992. Synthesis of a homogeneous series of ketomethylene arginyl pseudopeptides and application to low molecular weight hirudin-like thrombin inhibitors. *J Med Chem 35*:3331–3341.

DiMaio J, Gibbs B, Munn D, Lefebre J, Ni F, Konishi Y. 1990. Bifunctional thrombin inhibitors based on the sequence of hirudin 45–65. *J Biol Chem 265*:21698–21703.

DiMaio J, Gibbs B, Munn D, Lefebre J, Ni F, Konishi Y. 1991. A new class of potent thrombin inhibitors that incorporates a scissile pseudopeptide bond. *FEBS Lett 282*:47–52.

Erhlich HJ, Grinnell BW, Jaskunas SR, Esmon CT, Yan SB, Bang NV. 1990. Recombinant human protein C derivatives: Altered response to calcium resulting in enhanced activation by thrombin. *EMBO J 9*:2367–2373.

Esmon CT. 1989. The roles of protein C and thrombomodulin in the regulation of blood coagulation. *J Biol Chem 264*:4743–4746.

Fenton JW. 1981. Thrombin specificity. *Ann NY Acad Sci 370*:468–495.

Fenton JW. 1986. Thrombin. *Ann NY Acad Sci 485*:5–15.

Fusetani N, Matsunaga S, Matsumoto H, Takebayashi Y. 1990. Cyclotheonamide: Potent thrombin inhibitors from a marine sponge *Theonella sp.* *J Am Chem Soc 112*:7053–7054.

Grutter MG, Priestle JP, Rahuel J, Grossenbacher H, Bode W, Hofsteenge J, Stone SR. 1990. Crystal structure of the thrombin–hirudin complex: A novel mode of serine protease inhibition. *EMBO J 9*:2361–2365.

Hagihara M, Schreiber SL. 1992. Reassignment of stereochemistry and total synthesis of the thrombin inhibitor cyclotheonamide B. *J Am Chem Soc 114*:6570–6571.

Hendrickson WA. 1985. Stereochemically restrained refinement of macromolecular structures. *Methods Enzymol 115B*:252–270.

Howard AJ, Gilliland GL, Finzel BC, Poulos TL, Ohlendorf DH, Salemme FR. 1987. The use of an imaging proportional counter in macromolecular crystallography. *J Appl Crystallogr 20*:383–387.

Ishii K, Gerszten R, Zheng YW, Welsh JB, Turck CW, Coughlin SR. 1995. Determinants of thrombin receptor cleavage. *J Biol Chem 270*:16435–16440.

Jones TA. 1982. A graphics model building and refinement system for macromolecules. *J Appl Crystallogr 15*:23–31.

Kline T, Hammond C, Bourdan P, Maraganore J. 1991. Hirulog peptides with scissile bond replacements resistant to thrombin cleavage. *Biochem Biophys Res Commun 177*:1049–1055.

Le Bonniec BF, Esmon CT. 1991. Glu 192 → Gln substitution in thrombin mimics the catalytic switch induced by thrombomodulin. *Proc Natl Acad Sci USA 88*:7371–7375.

Lee AY, Hagihara M, Karmacharya R, Albers MW, Schreiber SL, Clardy J. 1993. Atomic structure of the trypsin–cyclotheonamide complex: Lessons for the design of serine protease inhibitors. *J Am Chem Soc 115*: 12619–12620.

Lewis SD, Ng AS, Baldwin JJ, Fusetani N, Naylor AM, Shafer JA. 1993. Inhibition of thrombin and other trypsin-like serine proteinases by cyclotheonamide A. *Thromb Res 70*:173–190.

Mann KG. 1994. Prothrombin and thrombin. In: Colman RW, Hirsh J, Marder VJ, Salzman EW, eds. *Hemostasis and Thrombosis: Basic Principles and Clinical Practice, 3rd ed.* Philadelphia, Pennsylvania: J.B. Lippencott, Co. pp 184–199.

Maraganore JM. 1993. Thrombin, thrombin inhibitors, and the arterial thrombotic process. *Thromb Haemostasis 70*:208–211.

Maraganore JM, Bourdon P, Jablonski J, Ramachandran KL, Fenton JW. 1990. Design and characterization of hirulogs: A novel class of bivalent peptide inhibitors of thrombin. *Biochemistry 29*:7095–7101.

Markwardt F. 1989. Development of hirudin as an antithrombotic agent. *Sem Thromb Haemost 15*:269–282.

Martin PD, Robertson W, Turk D, Huber R, Bode W, Edwards BFP. 1992. The structure of residues 7–16 of the Aα-chain of human fibrinogen bound to bovine thrombin at 2.3 Å resolution. *J Biol Chem 267*:7911–7920.

Maryanoff BE, Qiu X, Padmanabhan KP, Tulinsky A, Almond HR Jr, Andrade-Gordon P, Greco MN, Kaufman JA, Nicolaou KC, Liu A, Brung PH, Fusetani N. 1993. Molecular basis for the inhibition of human-thrombin by the macrocyclic peptide cyclotheonamide A. *Proc Natl Acad Sci USA 90*:8048–8052.

Mathews II, Padmanabhan KP, Ganesh V, Tulinsky A, Ishii M, Chen J, Turck CW, Coughlin SR, Fenton JW II. 1994. Crystallographic structures of thrombin complexed with thrombin receptor peptides: Existence of expected and novel binding modes. *Biochemistry 33*:3266–3279.

Morrison JF. 1982. The slow, tight-binding inhibition of enzyme-catalyzed reactions. *Trends Biochem Sci 7*:102–105.

Powers JC, Harper JW. 1986. Inhibitors of serine proteinases. In: Barrett AJ, Salvesen G, eds. *Proteinase inhibitors*. The Netherlands: Elsevier Science Publishers B.V. (Biomedical Division). pp 55–152.

Priestle JP, Rahuel J, Rink H, Tones M, Grutter MG. 1993. Changes in interactions in complexes of hirudin derivatives and human-thrombin due to different crystal forms. *Protein Sci 2*:1630–1642.

Qiu X, Padmanabhan KP, Carperos VE, Tulinsky A, Kline T, Maraganore JM, Fenton JW II. 1992. Structure of the hirulog 3-thrombin complex and nature of the S′ subsites of substrates and inhibitors. *Biochemistry 31*:11689–11697.

Qiu X, Yin M, Padmanabhan KP, Krstenansky JL, Tulinsky A. 1993. Structures of thrombin complexes with a designed and a natural exosite peptide inhibitor. *J Biol Chem 268*:20318–20326.

Rydel TJ, Ravichandran KG, Tulinsky A, Bode W, Huber R, Roitsch C, Fenton JW II. 1990. The structure of a complex of recombinant hirudin and human-thrombin. *Science 249*:277–280.

Rydel TJ, Tulinsky A, Bode W, Huber R. 1991. Refined structure of the hirudin–thrombin complex. *J Mol Biol 221*:583–601.

Sadler JE, Lentz SR, Sheehan JP, Tsiang M, Wu Q. 1993. Structure–function relationships of the thrombin–thrombomodulin interaction. *Haemostasis 23*:183–193.

Skrzypczak-Jankun E, Carperos VE, Ravichandran KG, Tulinsky A, Westbrook M, Maraganore JM. 1991. Structure of the hirugen and hirulog 1 complexes of thrombin. *J Mol Biol 221*:1379–1393.

Stenflo J, Fernlund P. 1982. Amino acid sequence of the heavy chain of protein C. *J Biol Chem 257*:12180–12190.

Stubbs MT, Oschkinat H, Mayr I, Huber R, Angliker H, Stone SR, Bode W. 1992. The interaction of thrombin with fibrinogen: A structural basis of its specificity. *Eur J Biochem 206*:187–193.

Szewczuk Z, Gibbs BF, Yue SY, Purisima E, Konishi Y. 1992. Conformationally restricted thrombin inhibitors resistant to proteolytic digestion. *Biochemistry 31*:9132–9140.

Szewczuk Z, Gibbs BF, Yue SY, Purisima E, Zdanov A, Cygler M, Konishi Y. 1993. Design of linker for trivalent thrombin inhibitors: Interaction of main chain of the linker with thrombin. *Biochemistry 32*:3396–3404.

Tulinsky A, Blevins RA. 1987. Structure of a tetrahedral transition state complex of an α-chymotrypsin dimer at 1.8 Å resolution. *J Biol Chem 262*: 7737–7742.

Tulinsky A, Qiu X. 1993. Active site and exosite binding of α-thrombin. *Blood Coag Fibrinolysis 4*:305–312.

Van Duyne GD, Standaert RF, Karplus PA, Schreiber SL, Clardy J. 1991. Atomic structure of FKBP–FK506, an immunophilin–immunosuppressant complex. *Science 252*:839–842.

Vijayalakshmi J, Padmanabhan KP, Mann KG, Tulinsky A. 1994. The isomorphous structures of prethrombin2, hirugen- and PPACK-thrombin: Changes accompanying activation and exosite binding. *Protein Sci 3*: 2254–2271.

Vu TKH, Hung DT, Wheaton VI, Coughlin SR. 1991a. Molecular cloning of a functional thrombin receptor reveals a novel proteolytic mechanism of receptor activation. *Cell 64*:1057–1068.

Vu TKH, Wheaton VI, Hung DT, Charo I, Coughlin SR. 1991b. Domains specifying thrombin-receptor interaction. *Nature 353*:674–677.

Wilcox JN, Rodriguez J, Subramanian R, Ollerenshaw J, Zhong C, Hayzer DJ, Horaist C, Hanson SR, Lumsen A, Salam TA, Kelly AB, Harker LA, Runge M. 1994. Characterization of thrombin receptor expression during vascular lesion formation. *Circ Res 75*:1029–1038.

Williams JW, Morrison JF. 1979. The kinetics of reversible tight-binding inhibition. *Methods Enzymol 63*:437–467.

Zdanov A, Wu S, DiMaio J, Konishi Y, Li Y, Wu X, Edwards BFP, Martin PD, Cygler M. 1993. Crystal structure of the complex of human α-thrombin and nonhydrolyzable bifunctional inhibitors, hirutonin-2 and hirutonin-6. *Proteins Struct Funct Genet 17*:252–265.